Fermi National Accelerator Laboratory

FN-356
2562.000

SATURATED AVALANCHE CALORIMETER

M. Atac
Fermi National Accelerator Laboratory

S. Kim
Tsukuba University

M. Mishina
KEK

W. Chinowsky, R. Ely, M. Gold, J. Kadyk
P. Rowson, K. Shinsky, and Y. Wong
Lawrence Berkeley Laboratory

R. Morse and M. Procario
University of Wisconsin

and
T. Schaad
Harvard University

February 8, 1982

FN-356
2562.000
February 8, 1982

SATURATED AVALANCHE CALORIMETER*

M. Atac
Fermi National Accelerator Laboratory

S. Kim
Tsukuba University

M. Mishina
KEK

W. Chinowsky, R. Ely, M. Gold, J. Kadyk
P. Rowson, K. Shinsky, and Y. Wong†
Lawrence Berkeley Laboratory

R. Morse and M. Procario
University of Wisconsin

T. Schaad
Harvard University

Abstract

A gas sampling electromagnetic calorimeter running in a "Saturated Avalanche Mode" was tested at SLAC with positrons incident at energy up to 17.5 GeV. With this new method, good energy resolution, 16 percent/$\sqrt{E}$, and good linearity were obtained with arrays of thirty-four 0.5 radiation length thick lead plates interleaved with 34 wire counters. There was no measurable systematic effect. Amplifiers are not needed; the signals are large enough to be connected directly to the ADC's.

†Present address: Institute of HEP, Ac. Sinica, Beijing, P. R. China

*Presented at the 2nd Topical Conference on Forward Collider Physics, Madison, Wisconsin (December 1981).

Introduction

Gas sampling calorimeters operating in a proportional mode have been tested and used by several groups[1-10] but, with one reported exception[6], their energy resolution has been much inferior to that achieved with calorimeters that use plastic scintillator counters. Improved resolution has been demonstrated in a calorimeter operated in the Geiger mode[11], and may be expected also with the limited streamer[12, 13] mode. Those devices are intrinsically different from proportional counter energy sampling calorimeters. The former, in effect, use the number of tracks in the shower, while the latter use the magnitude of total collected charge as measures of the energy deposited in the gas. In this paper, we report results of tests of gas sampling calorimeters run in neither of these modes, but in an intermediate, partially saturated mode. Their resolution is comparable to that of plastic scintillator calorimeters.

These tests were made as part of the program to develop calorimeter modules for the Collider detector facility[14], as apparatus to detect products of $\bar{p}p$ interactions at the 2 TeV colliding beams machine now under construction at Fermilab. The present design (Fig. 1) calls for gas sampling electromagnetic and hadronic calorimetry in the forward and backward angular regions. Respectably small granularity will be achieved with tower structures of cathode readout pads.

Experimental Arrangements

Two detectors studied were a MAC prototype[6] and brass tube calorimeter[10] (BTC) which were tested previously in proportional mode at SLAC and at Fermilab, respectively. Thus, only limited details of construction will be given here.

The MAC prototype was composed of 34 lead plates of 2.8 mm thickness and 34 planes of 50 μm diameter anode wires enclosed in 9.5 mm x 9.5 mm cells which are separated by 1.5 mm thick aluminum ribs, a 17.8 radiation length shower detector. Fig. 2 shows the arrangement and the cell structure. Both detectors were individually placed in aluminum containers which could be evacuated or pressurized for studying pressure effects. The anode wires of each plane were connected to a common strip, and seven such planes were further grouped together, resulting in five groups to be read out. Most of the results that will be presented in this paper were obtained from the total sum of these five groups. Results on the longitudinal development in the shower will be reported later.

The counter gas was a mixture of 49.3 percent Argon, 49.3 percent ethane, and 1.4 percent ethyl alcohol. Negative high voltage was applied to the cathode tubes. Distributed high voltage capacitors totalling 0.25 μf were the charge storage elements. As indicated in the figure, there was no need for amplifiers between the wires and the ADC's. Indeed, it was necessary to attenuate the large signals obtained between 2 db and 30 db depending on the high voltage and gas pressure. Forty meters of RG58 coaxial cables carried the signals to the LeCroy 2249W ADC's. The ADC pedestals were determined with a linear extrapolation of the measured variation of pulse height

The wires of the BTC were connected together longitudinally, as shown in Fig. 3, and further grouped as indicated above and in the figure. The BTC was made of 0.36 mm wall thickness, 6.3 mm x 11.3 mm cross section brass tubes containing 50 μm diameter anode wires. Forty 2-mm thick lead plates were between the wire planes to give a total of 16.5 radiation lengths.

A LSI-11 computer system with a SLAC program package "ATROPOS" was used for data taking and on-line display and monitoring.

Beam Parameters

The detectors were tested in the 19° beam of the Stanford Linear Accelerator which provided positrons of 17.5 GeV maximum energy. SLAC ran in the SLED mode during the entire tests with a bunch length of about 20 nsec, FWHM 8 nsec, and 10 bunches per second. About 95 percent of the beam at the detector was within the 2 mm x 2 mm area of the beam defining counter. The intensity was, on the average, between 1/10 and 10 positrons per bunch. The momentum spread of the beam, $\Delta p/p$ was less than ±0.25 percent rms.

Experimental Results

Most of the data presented here were taken with the MAC prototype calorimeter. Gain and resolution were measured at various settings of gas pressure and applied voltage with positrons incident at selected energies in the range 1.5 GeV-17.5 GeV available in the SLAC test beam. A representative sample of typical results will be shown.

For 10 GeV incident positrons, the total pulse height distribution is shown in Fig. 4 together with a Gaussian fit to the data. Only that portion of the distribution within $\pm 2\sigma$ of the mean were used in the fitting procedure. The shape of the distribution, typical of all, is well represented by the Gaussian function.

With fixed gas pressure, the resolution σ/E varies with high voltage as shown in Fig. 5. As the voltage increases from 2100 V, the resolution slowly decreases to a shallow minimum at $\sim$ 2250 V and then slowly increases.

Figs. 6a and 6b present the calorimeter output as a function of incident positron energy. Both at 0 psig and 5 psig there is no departure from linearity at energies up to 17.5 GeV. For these runs, the counters were run at 2300 V and 2550 V, respectively.

Fig. 7 shows the total pulse height as a function of high voltage for the pressures of 0 psig and 3 psig. Both show approximately exponential rise in gain with increasing voltage. The higher pressure curve has some indication of an inflection point near the middle of the range.

Higher energy response of the detector was simulated by using multiple positrons in a single rf bucket. This is a fair simulation since the positive ions do not move appreciably from where they were produced during the beam spill. Fig. 8 shows the detector response to multiple positrons of 17.5 GeV. It shows that as many as 11 simultaneous positrons the energy resolution of the detector is sufficiently good to resolve them with clear minima between the peaks of the pulse height distributions for the corresponding numbers of positrons. In fact, this is a Poisson distribution for $n = 4.5$. The oscilloscope trace reproduced in Fig. 9 shows some pulses for single and

double positrons. The pulse rise time is about 10 nsec, and the decay time is almost 800 nsec. The decay time is long because the whole detector whose capacitance exceeds 10 nF was connected to a single 50 Ω coaxial cable. The pulse height for singles is ∿ 75 mV and is ∿ 150 mV for doubles. These pulses can be used for a prompt multiplicity trigger with a time jitter of few nanoseconds. That the pulse height for the multiple positrons deviate in a smooth way from linear behavior for more than 2 positron (35 GeV) shower is seen in Figs. 10a and b. The linearity is much better at 8 psig. An expanded view of the pulse height distribution for 10 GeV positrons is shown in Fig. 11. It dramatically shows the symmetric, Gaussian-like shapes with clean valleys between the multiple-hit peaks. The energy resolution as a function of equivalent energy deposits of multiple 17.5 GeV positrons is shown in Fig. 12 after correction for the non-linear response.

The energy resolution as a function of energy for single incident positrons is shown in Fig. 13. σ/E shows the usual $E^{-1/2}$ dependence with a constant factor of 16.2 percent as indicated in Fig. 14. The shape of the dependence of resolution on energy indicates no systematic term since it extrapolates to the origin. This is, perhaps, because there is no active device (amplifier, pulse shaper, etc.) between the detector and the ADC, and small variations among individual wire gains average out over the detector.

The detector was rotated to make angles to the beam axis of as much as 23°. With 17.5 GeV positrons incident, the results of Fig. 15 were obtained. It is seen that the pulse height increases by a small amount (maximum 2.3 percent), and the σ/E decreases slightly with increasing angle. This improvement may be due to a better containment of energy in the effective thickness of the angled calorimeter.

Similar results were obtained from the BTC. It was run only above atmospheric pressure, 6 psig, because of the small distance, 3.5 mm, from the anode wire to the cathode tube wall. Fig. 16 shows that the energy resolution is almost 17 percent/$\sqrt{E}$ and independent of high voltage, in contrast to the behavior of the MAC prototype. The reason for the differences between the two may be the different cell shapes. It is curious that poorer resolution was found with the thinner lead sampling sheets. When this detector was tested at Fermilab in the proportional mode, the resolution was measured to be 22 percent/$\sqrt{E}$.

Saturated Avalanche Mode

We have investigated the ionization region[12] between the proportional region and the self quenching streamer region in detail using a 9.5 mm x 9.5 mm tube having a 50 μm wire, a replica of one cell of the prototype MAC detector, in order to understand the improved energy resolution of the apparatus relative to calorimeters running in the proportional mode.

A small fraction of the wire pulse was amplified and used to form the ADC trigger, as shown in Fig. 17. A LeCroy 2285 ADC system was used for measuring the charge. The gain of the ADC was 20 counts per picocoulomb. An Fe^{55} x-ray source was used to measure the wire gain as a function of high voltage. As seen in Fig. 19 a and b, the resolution is insufficient to separate the 5.9 keV x-ray line and 2.9 keV argon escape line when the gas gain, at 2300 V, is in the region of limited proportionality. The gain here was $\sim 5 \times 10^4$. The 2.9 keV line is hidden in the left side of the asymmetric pulse height distribution. Fig. 20 shows the gain as a function of the high

voltage. The rate of growth of the avalanche is seen to decrease continuously as the high voltage increases above 2200 V until the streamer threshold is reached. Then the gain increases very little to the point of full streamer operation around 2650 V.

The distribution of pulse heights recorded by passage of minimum ionization tracks was also investigated in this voltage region using a Sr^{90} β-source. A telescope made from a pair of small thin scintillation counters provided a gate pulse for the ADC's. The discriminator thresholds were set to accept mainly the minimum ionizing β's. Fig. 20a shows the pulse height distribution obtained at 2300 V. This histogram shows that the distribution is almost symmetric with a small tail. The distribution made by the β's is not like a typical Landau distribution obtained in a gas gap of 9.5 mm thickness at atmospheric pressure. The tail is greatly suppressed. An expanded view of the histogram of Figs 20a is shown in Fig. 20b. It has a ratio of σ to mean of 34 percent. Landau fluctuations clearly have been reduced, an indication that the greater the concentration of primary ionization, the more saturation (less gain) occurs as has been observed earlier[15].

From the data of Fig. 18, we find a ratio of mean pulse heights produced by the two photons of $\sim$ 1.4, rather than the $\sim$ 2.0 ratio of energies. Similar conclusions about the departure from strict linear, proportional response follows from comparison of the signals from the β and x-ray sources. Those observations and the suppression of the Landau tail indicate partial saturation of the avalanche charge at the collecting wire. Thus, the resolution is improved compared to that obtained when the counters operate in the proportional mode. We find a resolution somewhat smaller than, but not really inconsistent

with that predicted by Fischer[16], which is based on a calculation of the response without the effect of Landau fluctuations. Deterioration in resolution at voltages much higher than 2400 V may be caused by fluctuations in gain where streamer and saturated avalanche modes overlap (see Fig. 19). Depending on the amount of ionization deposited locally on the wire, the gain may be low (saturated avalanche) or more than an order of magnitude higher (streamer).

Acknowledgments

The authors express their appreciation to Drs. R. Coombes, R. Prepost, and D. M. Ritson for providing the MAC prototype; to Drs. R. Schwitters and A. Tollestrup for support; to Dr. R. Gearhart and the SLAC operating crew for assisting and supporting the runs; to P. Clancy and S. Mackenzie for help with the data acquisition system; and to M. Hrycyk for modifying the BTC.

References

Ref. 1 W. Murzin, Progr. Element. Part. Cosmic Ray Phys. (1967) 245.

Ref. 2 M. E. Nordberg, Jr., Cornell Univ. Report, CLNS 138 (1971).

Ref. 3 T. Kotsura et al., Nucl. Instr. and Meth. 105 (1972) 245.

Ref. 4 M. Atac, IEEE Trans. on Nucl. Sci., Vol. NS-28, No. 1, Feb. 1981.

Ref. 5 M. Atac et al., IEEE Trans. on Nucl. Sci., Vol. NS-28, No. 1, Feb. 1981.

Ref. 6 R. L. Anderson et al., IEEE Trans. on Nucl. Sci., Vol. NS-25 (1978) 340.

Ref. 7 C. Bosio et al., Nucl. Instr. and Meth. 157 (1978) 35.

Ref. 8 P. Skubic et al., IEEE Trans. on Nucl. Sci., Vol. NS-28, No. 1, Feb. 1981.

Ref. 9 H. Tyco et al., UCLA Report.

Ref. 10 M. Mishina et al., IEEE Trans. on Nucl. Sci. (Feb. 1982).

Ref. 11 W. Carithers et al., private communication; will be published in Nucl. Instr. and Meth.

Ref. 12 M. Atac et al., Fermilab Report FN-337 (1981), and Proc. of INS International Symp. on Nucl. Radiation Detectors (March 1981), Tokyo.

Ref. 13 M. Jonker et al., Physica Scripta Vol. 23, 677-679, 1981.

Ref. 14 Fermlab $\bar{p}p$ Colliding Detector Proposal (1979).

Ref. 15 H. Frehse et al., Nucl. Instr. and Meth. 156 (1978) 87.

Ref. 16 G. Fischer, Nucl. Instr. and Meth. 156 (1978) 81.

Figure Captions

Fig. 1 — A cross section view of the Collider Detector Facility at Fermilab.

Fig. 2 — The experimental configuration of the MAC electromagnetic calorimeter.

Fig. 3 — The experimental configuration of the brass tube electromagnetic calorimeter.

Fig. 4 — A typical pulse height distribution and Gaussian fitted points for obtaining σ and mean values using 2σ fit.

Fig. 5 — σ/E versus high voltage for 10 GeV positrons at 0 psig.

Fig. 6a and b — The total pulse height response of the calorimeter as function of the e^+ energy for 0 psig and 5 psig, respectively. The linearity is excellent for both pressures.

Fig. 7 — The total pulse height as a function of the high voltage for pressures of 0 psig and 3 psig.

Fig. 8 — The response of the detector to simultaneous multiple positrons of 17.5 GeV.

Fig. 9 — The oscilloscope picture of some single and double 17.5 GeV positron pulses.

Fig. 10a and b — The pulse heights as a function of simultaneous 17.5 GeV multiple positrons for 0 psig and 8 psig.

Fig. 11 — Pulse height distributions for 10 GeV multiple positrons.

Fig. 12 — $\sigma/\sqrt{E}$ versus simultaneous multiple 17.5 GeV positrons after correction for non-linear response.

Fig. 13 — σ/E versus positron energy.

Fig. 14 — σ/E versus $E^{-1/2}$ indicating no systematic effects.

Fig. 15 — Total pulse height and σ/E versus incident beam angle for 17.5 GeV positrons.

Fig. 16 — $\sigma/\sqrt{E}$ versus the high voltage for the brass tube calorimeter.

Fig. 17 — The circuit diagram for investigating the saturated avalanche region.

Fig. 18 — Pulse height distributions for the 5.9 x-rays from Fe^{55}. Fig. 18a shows the ADC distribution without amplifier. Note the 3 keV argon escape line is not visible in the saturated avalanche region because of poor proportionality. Fig. 18b shows the amplified distribution where the escape line is just visible because of the better resolution at high pulse heights.

Fig. 19 — The model tube gain as a function of the high voltage in the saturated avalanche region using the ADC without amplifier.

Fig. 20a and b — The pulse height distribution for minimum ionizing tracks in the saturated avalanche region showing almost symmetric distribution with very small Landau tail. Fig. 20b is the expanded detail of the Fig. 20a.

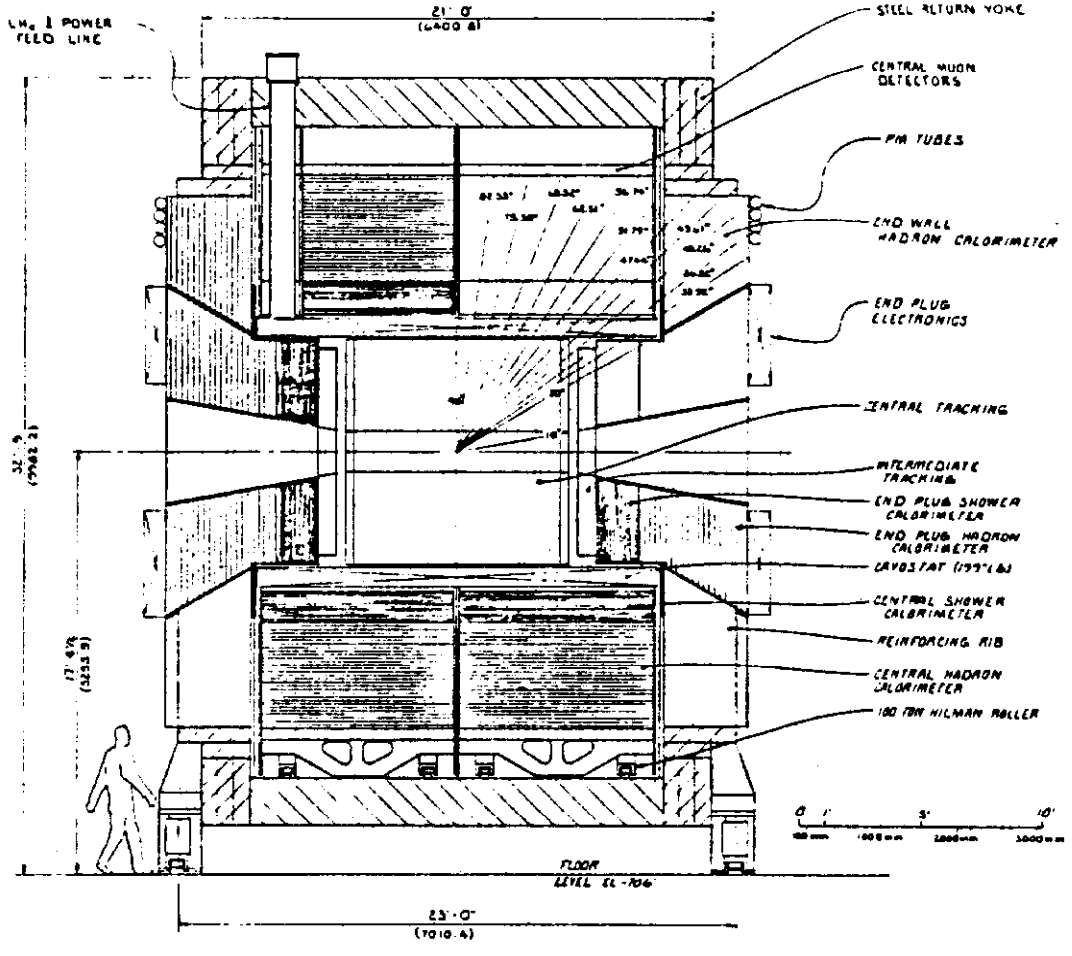
STEEL RETURN YOKE
CENTRAL MUON DETECTORS
PM TUBES
END WALL HADRON CALORIMETER
END PLUG ELECTRONICS
CENTRAL TRACKING
INTERMEDIATE TRACKING
END PLUG SHOWER CALORIMETER
END PLUG HADRON CALORIMETER
CENTRAL SHOWER CALORIMETER
REINFORCING RIB
CENTRAL HADRON CALORIMETER
FLOOR LEVEL EL -706'

FIG. 1

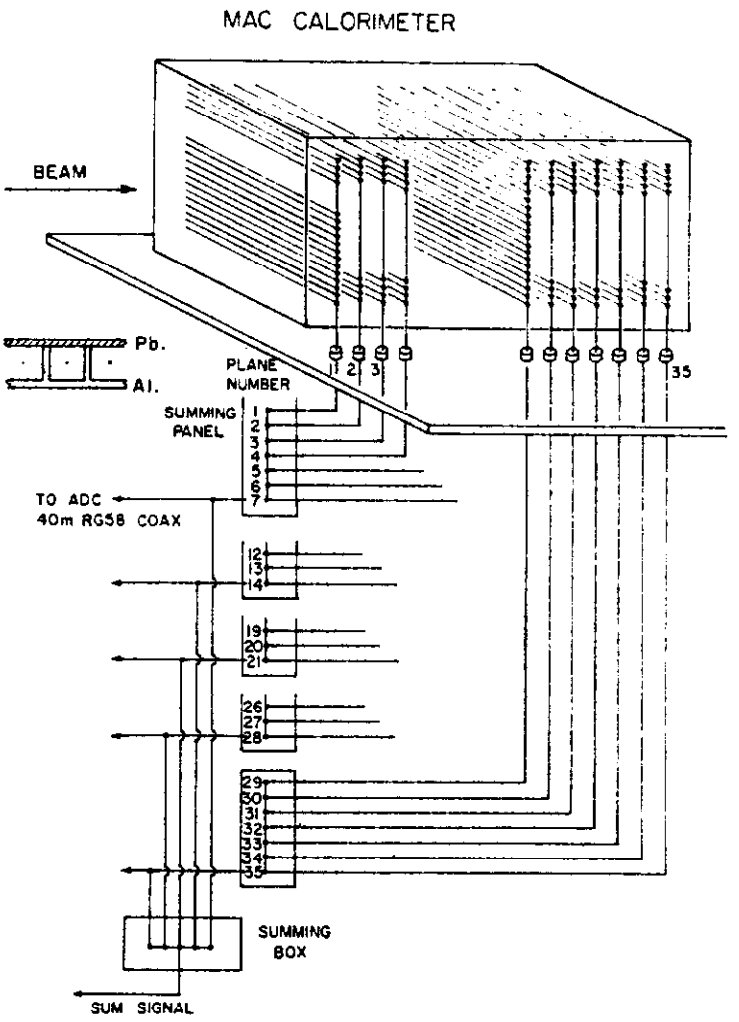
MAC CALORIMETER
BEAM
Pb.
Al.
PLANE NUMBER
1 2 3
35
SUMMING PANEL
1
2
3
4
5
6
7
TO ADC
40m RG58 COAX
12
13
14
19
20
21
26
27
28
29
30
31
32
33
34
35
SUMMING BOX
SUM SIGNAL

FIG. 2

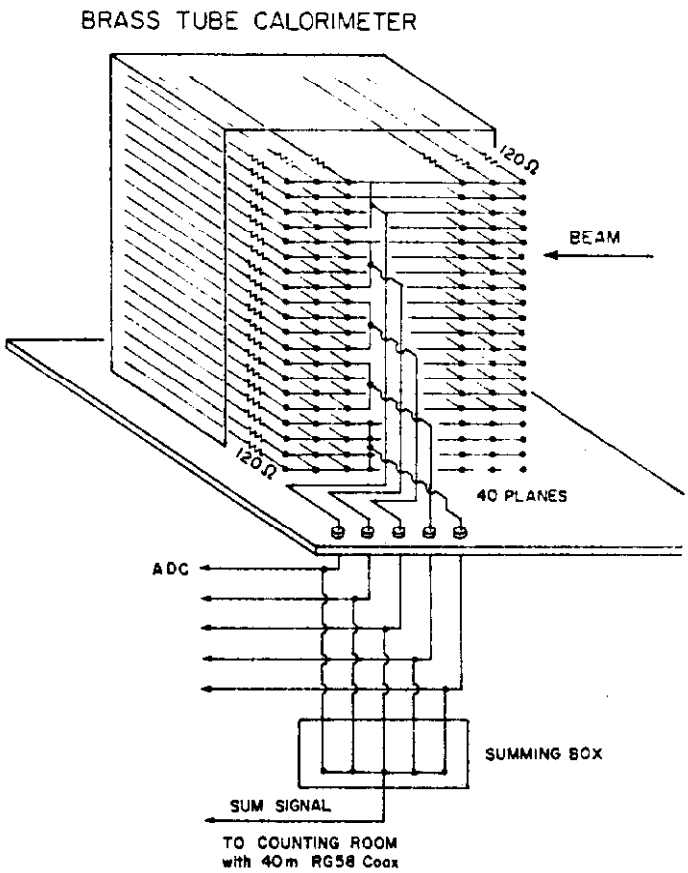
BRASS TUBE CALORIMETER
120Ω
BEAM
120Ω
40 PLANES
ADC
SUMMING BOX
SUM SIGNAL
TO COUNTING ROOM
with 40m RG58 Coax

FIG. 3

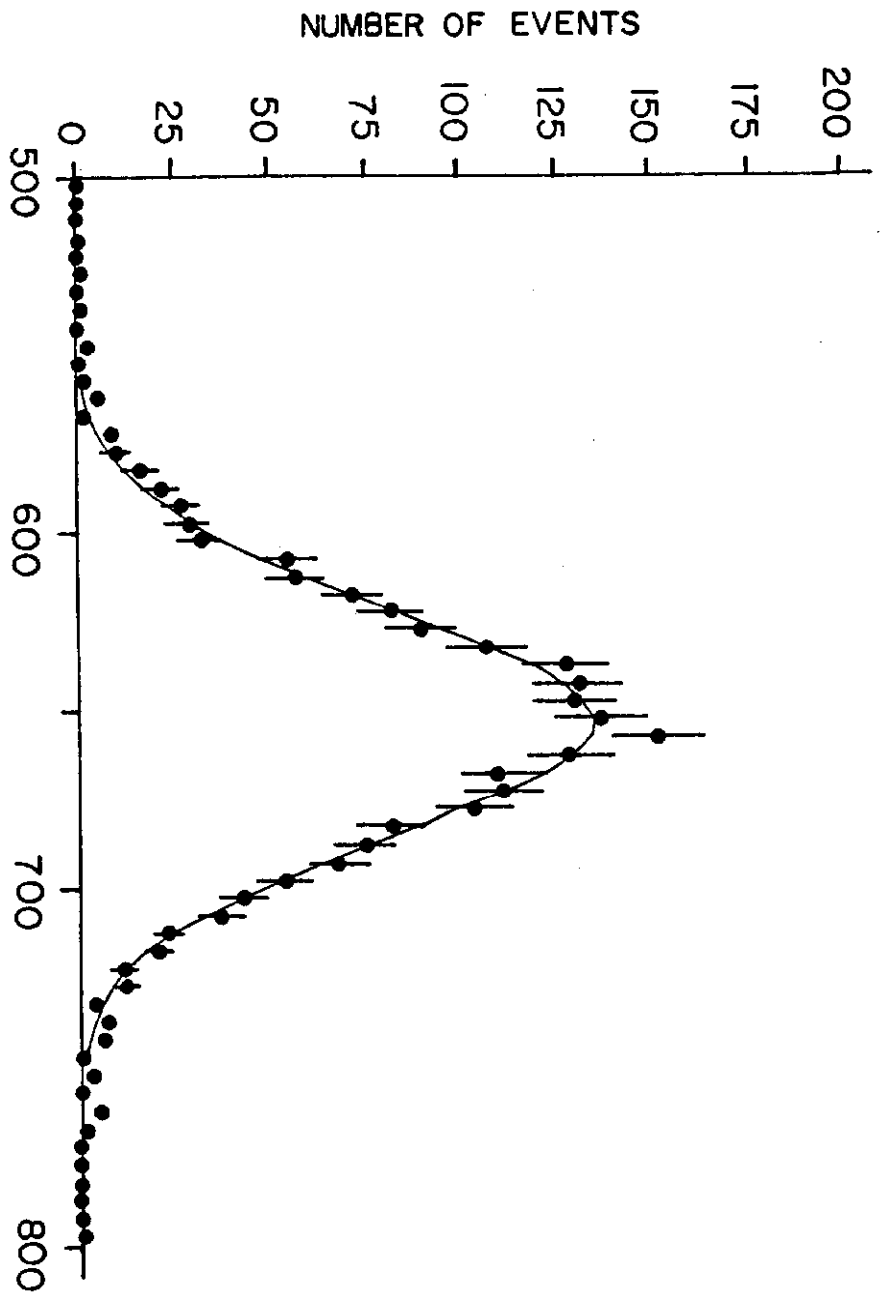
NUMBER OF EVENTS
0
25
50
75
100
125
150
175
200
500
600
700
800
ADC COUNT

FIG. 4

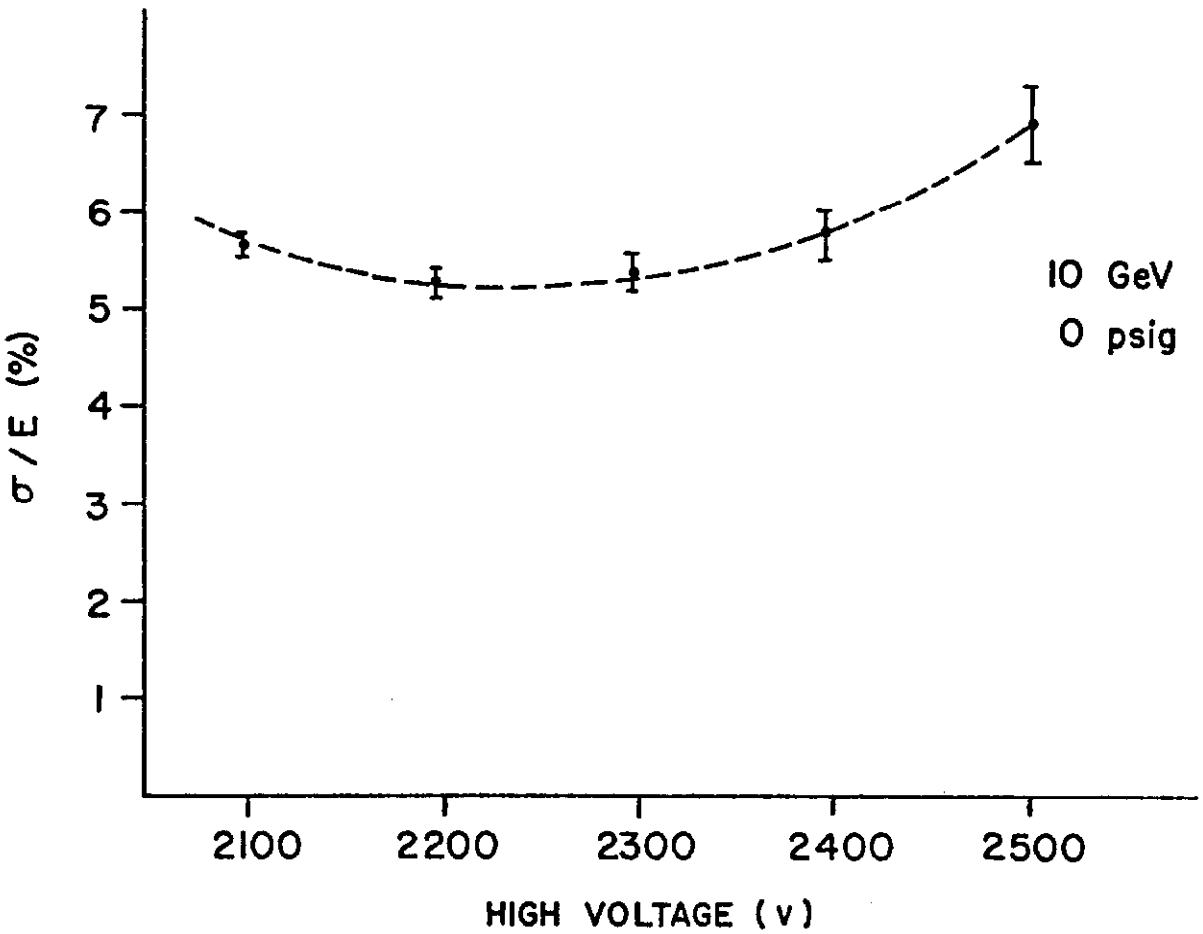
7
6
5
4
3
2
1
σ / E (%)
10 GeV
0 psig
2100
2200
2300
2400
2500
HIGH VOLTAGE (v)

FIG. 5

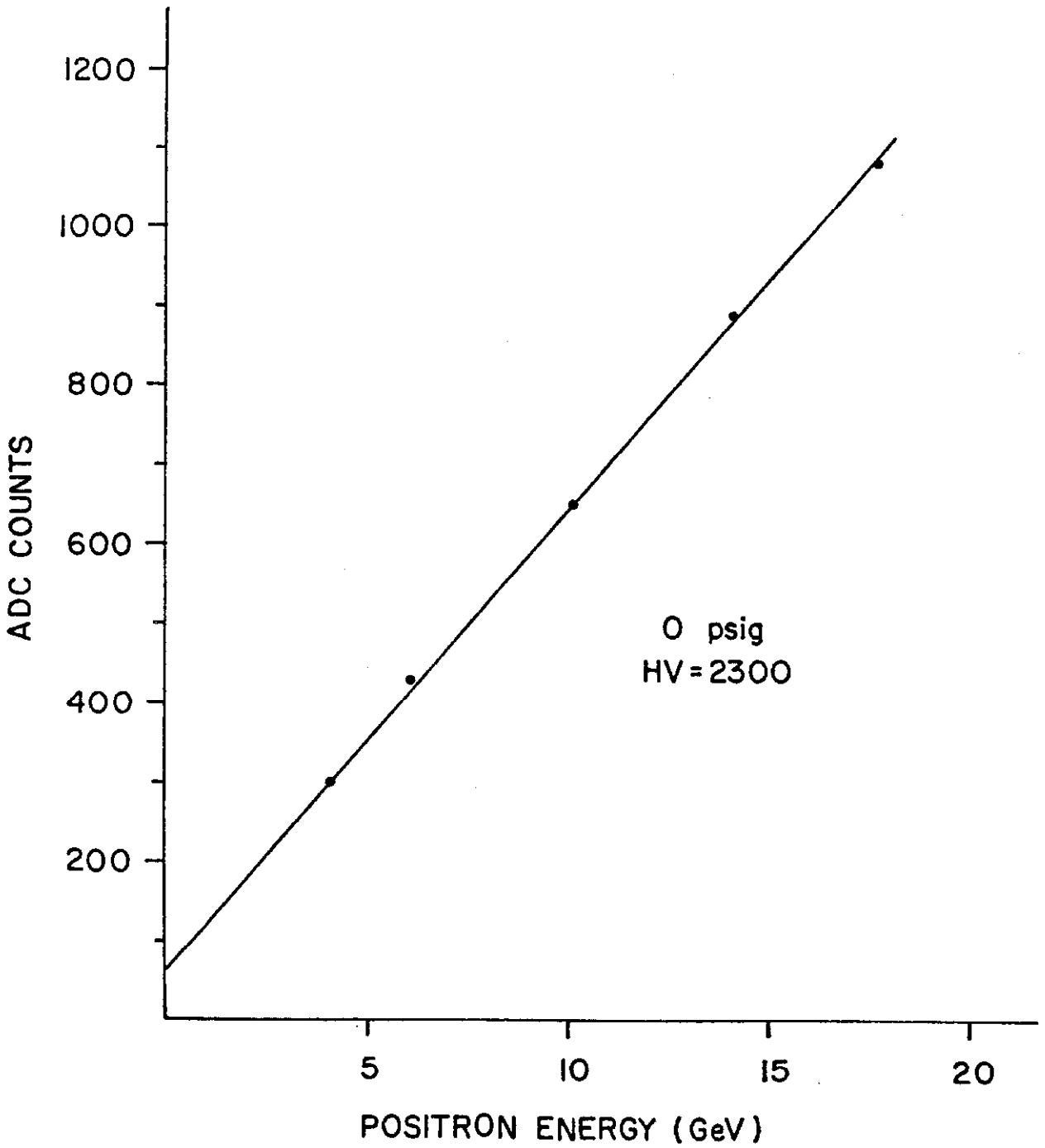
1200
1000
800
600
400
200
ADC COUNTS
0 psig
HV = 2300
5
10
15
20
POSITRON ENERGY (GeV)

FIG. 6a

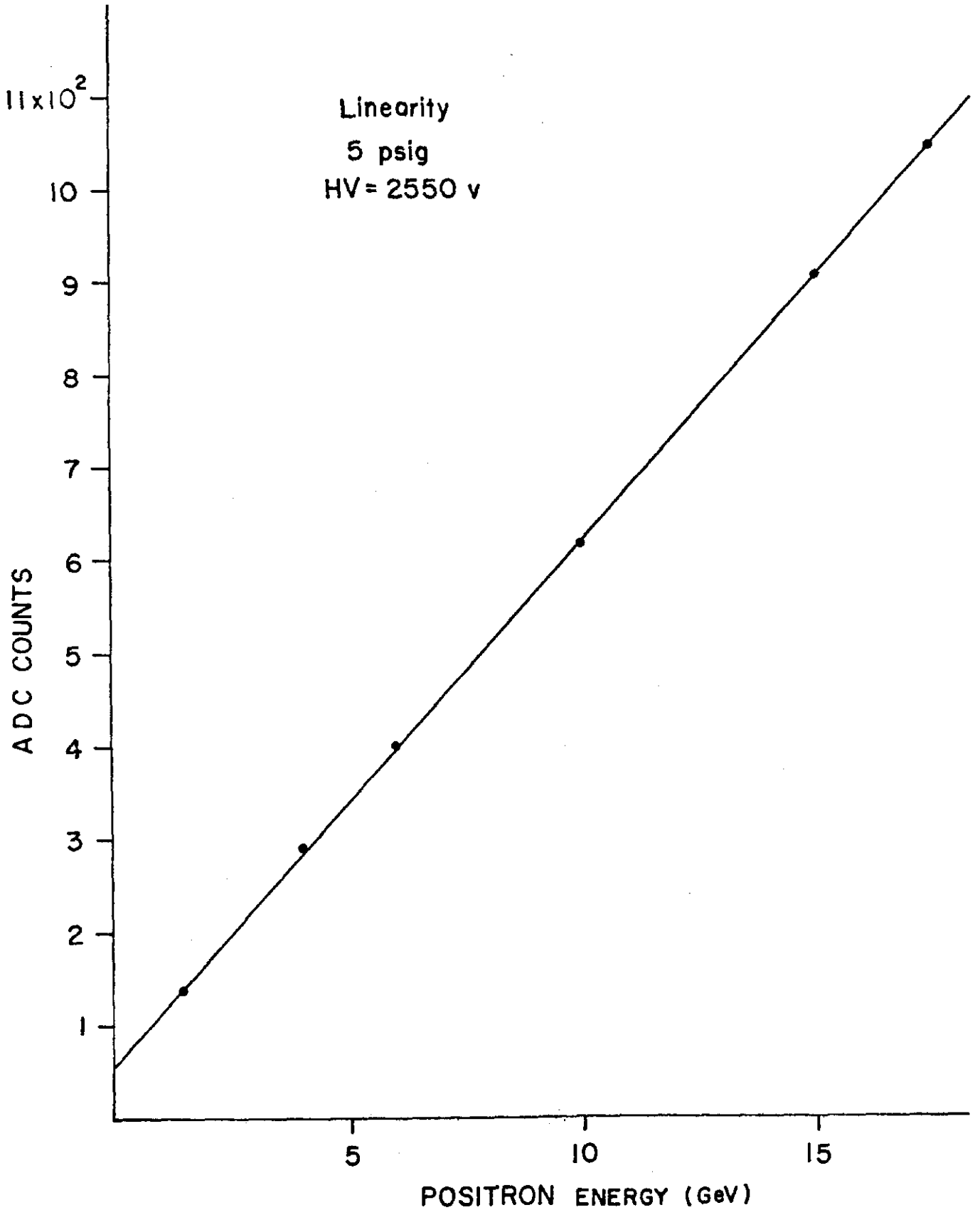
Linearity
5 psig
HV = 2550 v
11x10²
10
9
8
7
6
5
4
3
2
1
ADC COUNTS
5
10
15
POSITRON ENERGY (GeV)

FIG. 6b

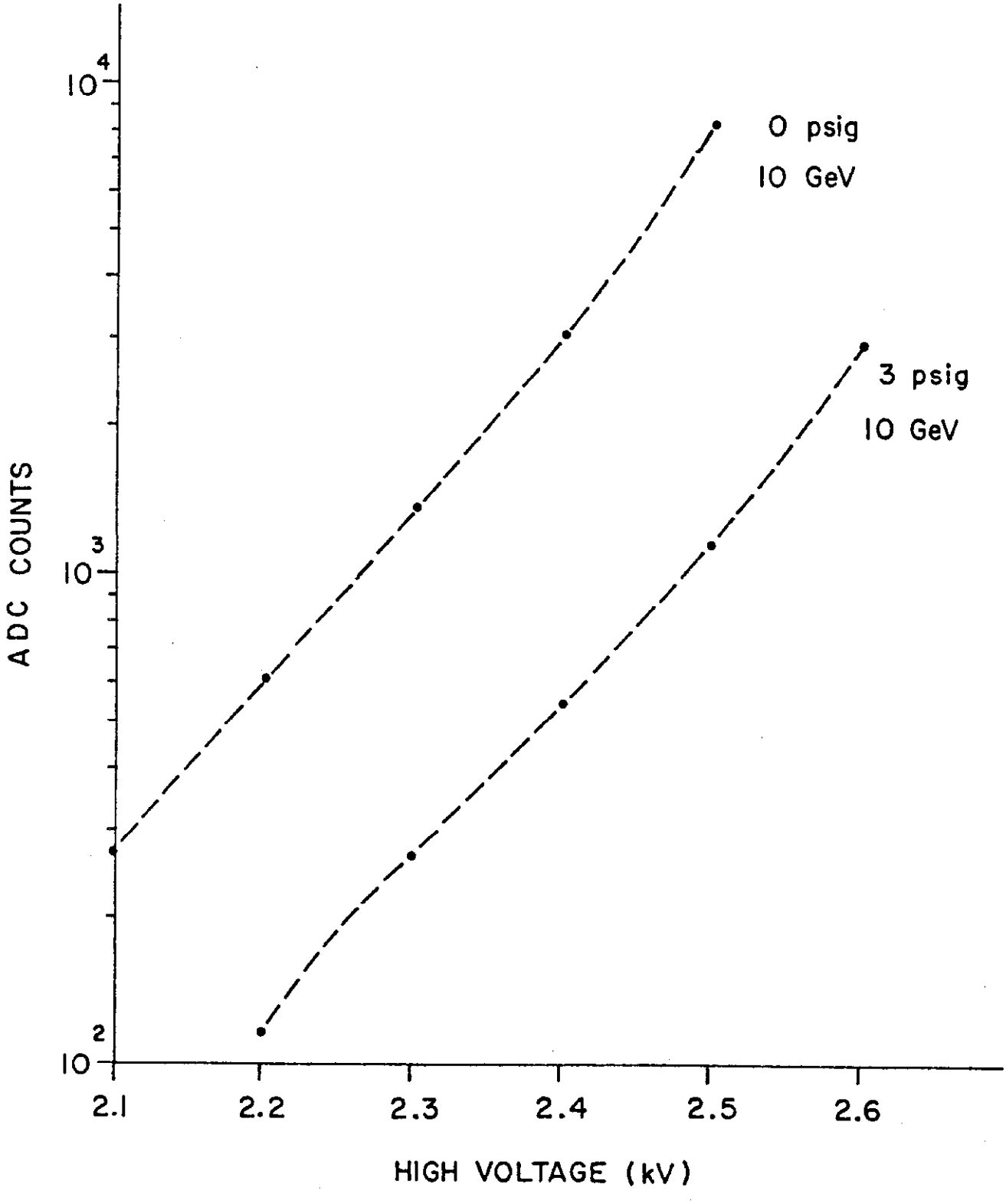
ADC COUNTS
10^4
10^3
10^2
0 psig
10 GeV
3 psig
10 GeV
2.1
2.2
2.3
2.4
2.5
2.6
HIGH VOLTAGE (kV)

FIG. 7

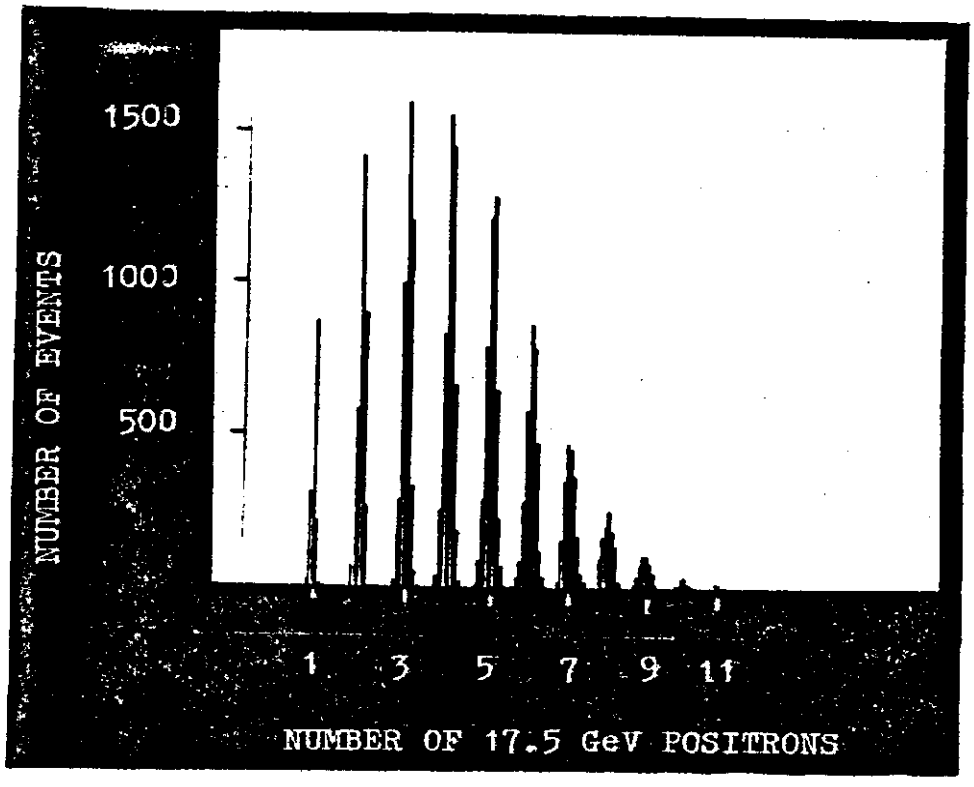
1500
1000
500
NUMBER OF EVENTS
1
3
5
7
9
11
NUMBER OF 17.5 GeV POSITRONS

FIG. 8

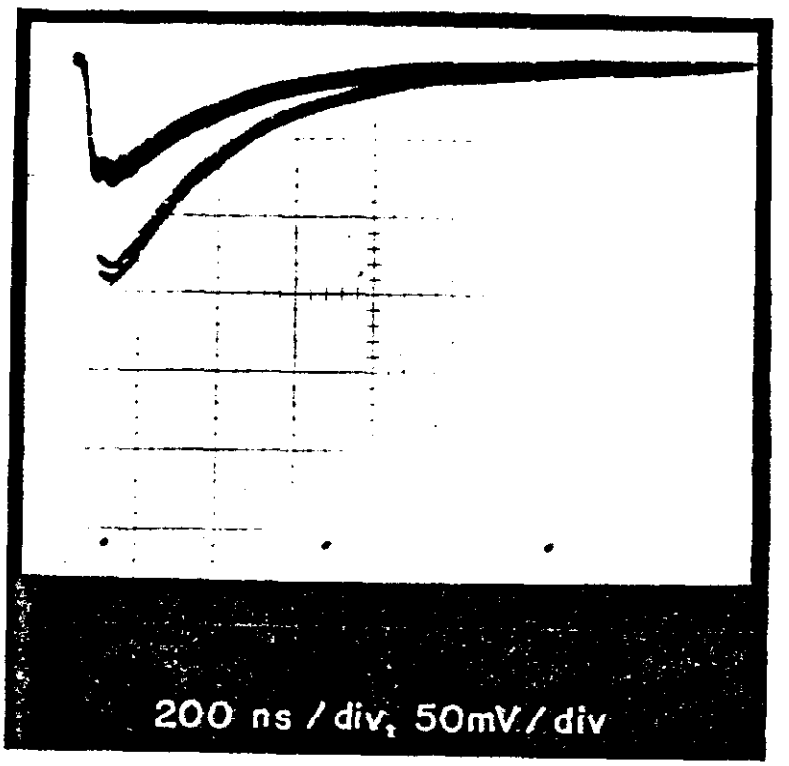

FIG. 9

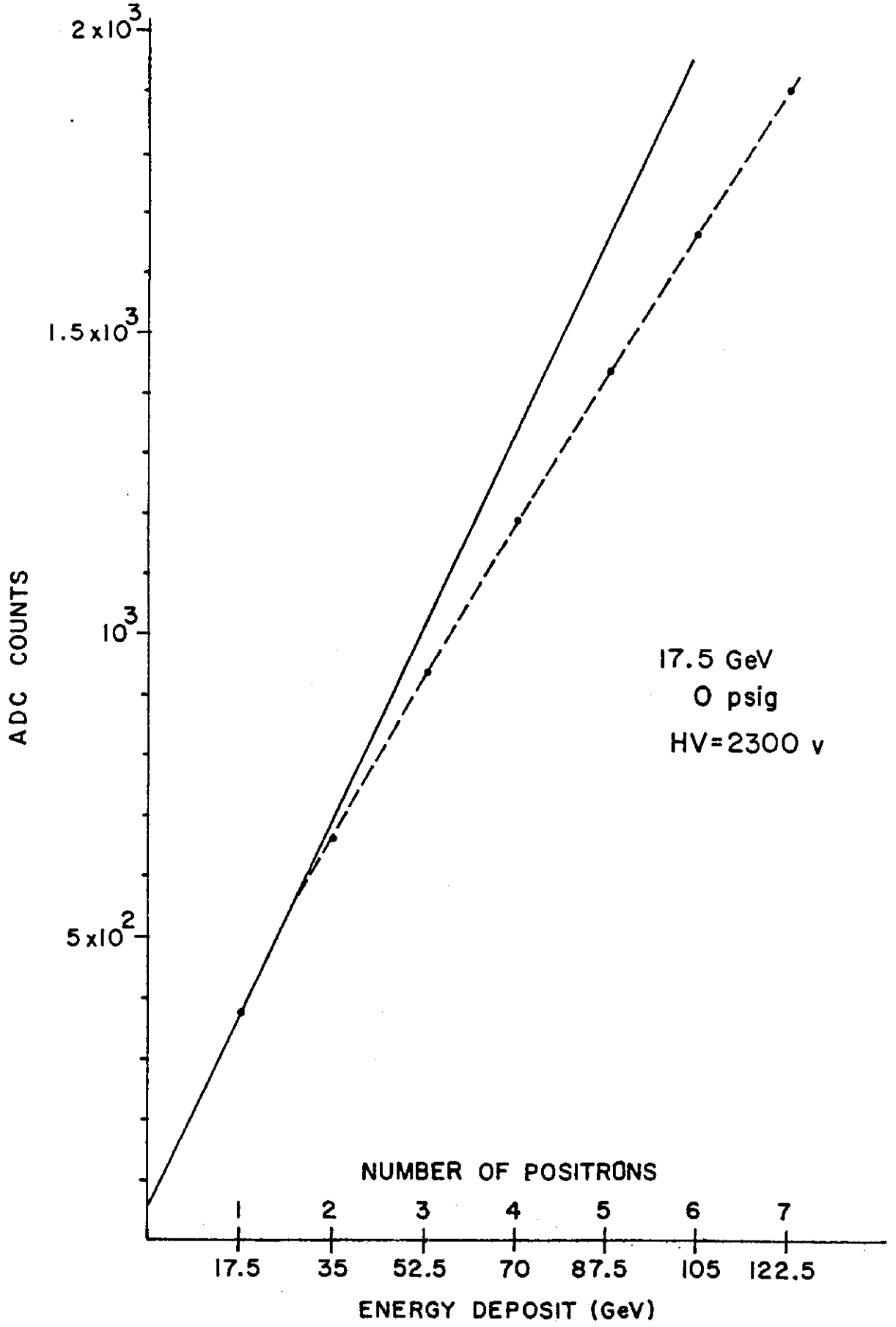
2x10^3
1.5x10^3
10^3
5x10^2
ADC COUNTS
17.5 GeV
0 psig
HV=2300 v
NUMBER OF POSITRONS
1
2
3
4
5
6
7
17.5
35
52.5
70
87.5
105
122.5
ENERGY DEPOSIT (GeV)

FIG. 10a

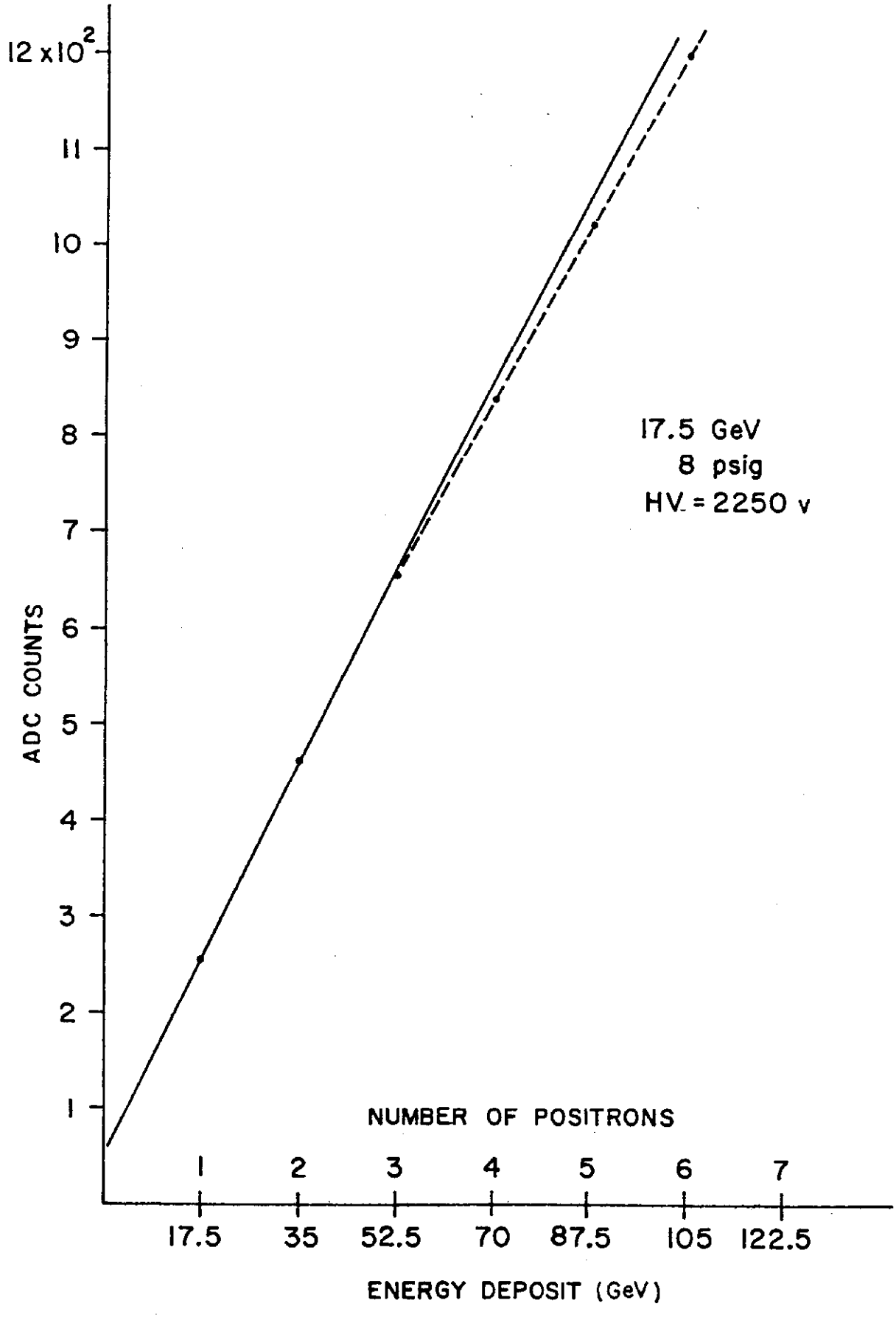
12 x 10²
11
10
9
8
7
6
5
4
3
2
1
ADC COUNTS
17.5 GeV
8 psig
HV = 2250 v
NUMBER OF POSITRONS
1
2
3
4
5
6
7
17.5
35
52.5
70
87.5
105
122.5
ENERGY DEPOSIT (GeV)

FIG. 10b

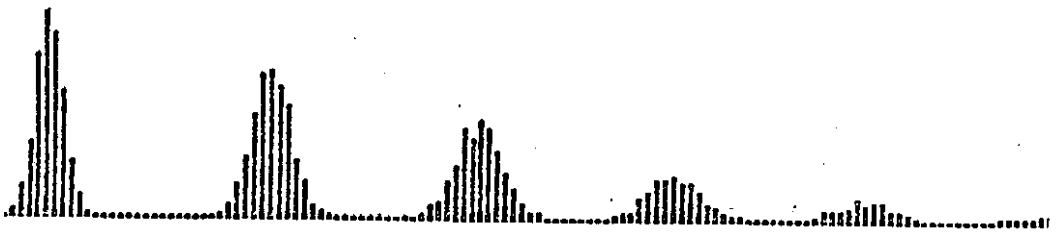

FIG. 11

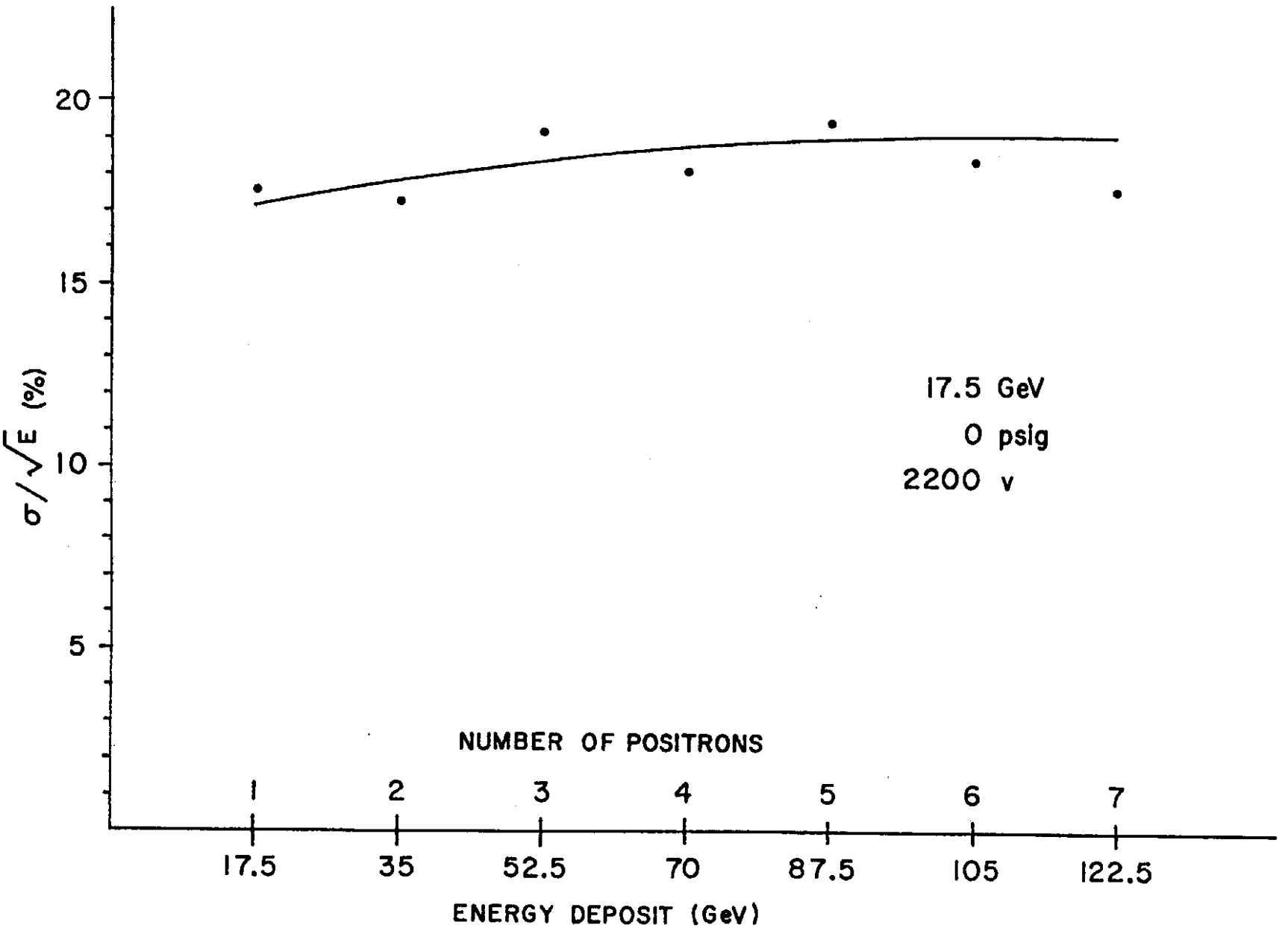
20
15
10
5
$\sigma/\sqrt{E}$ (%)
17.5 GeV
0 psig
2200 v
NUMBER OF POSITRONS
1
2
3
4
5
6
7
17.5
35
52.5
70
87.5
105
122.5
ENERGY DEPOSIT (GeV)

FIG. 12

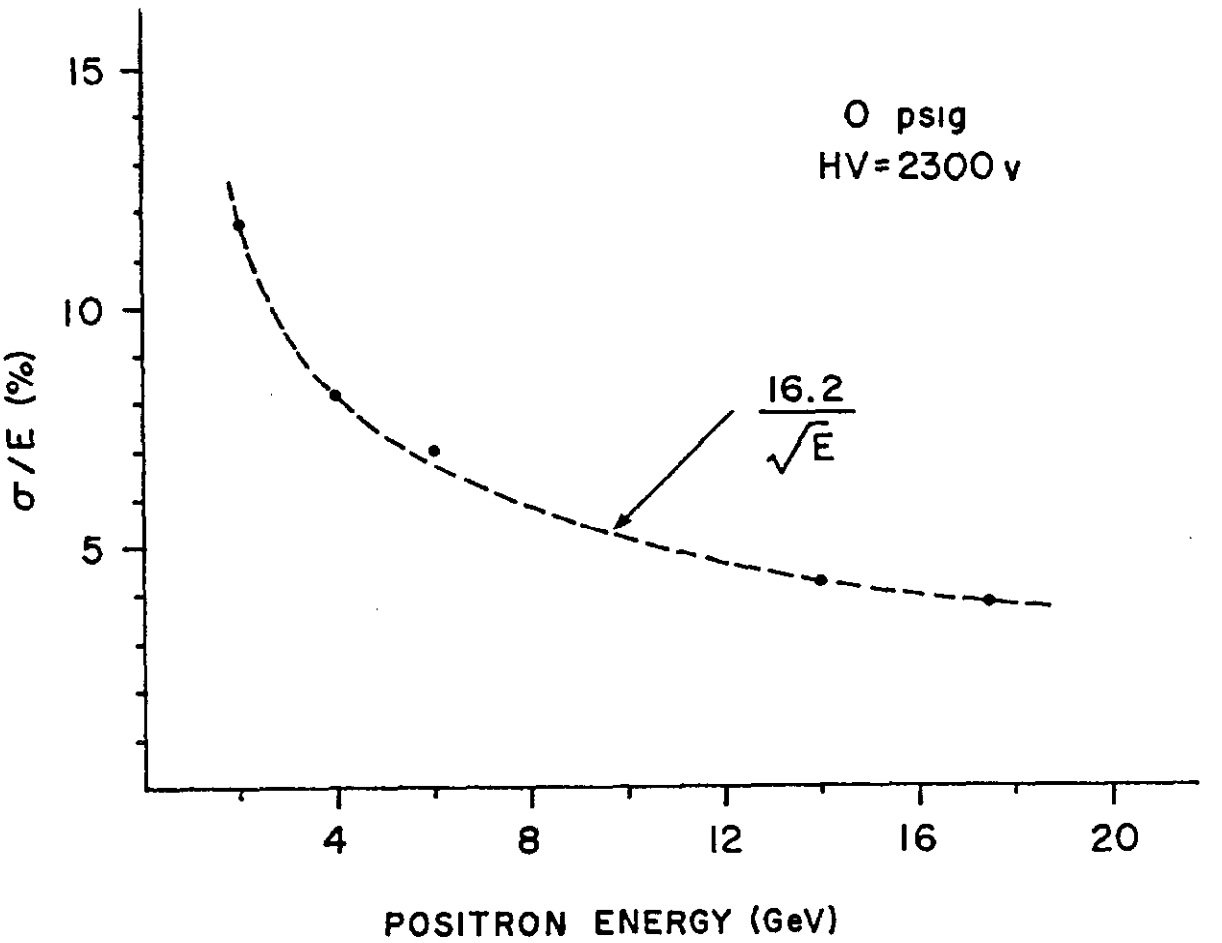

FIG. 13

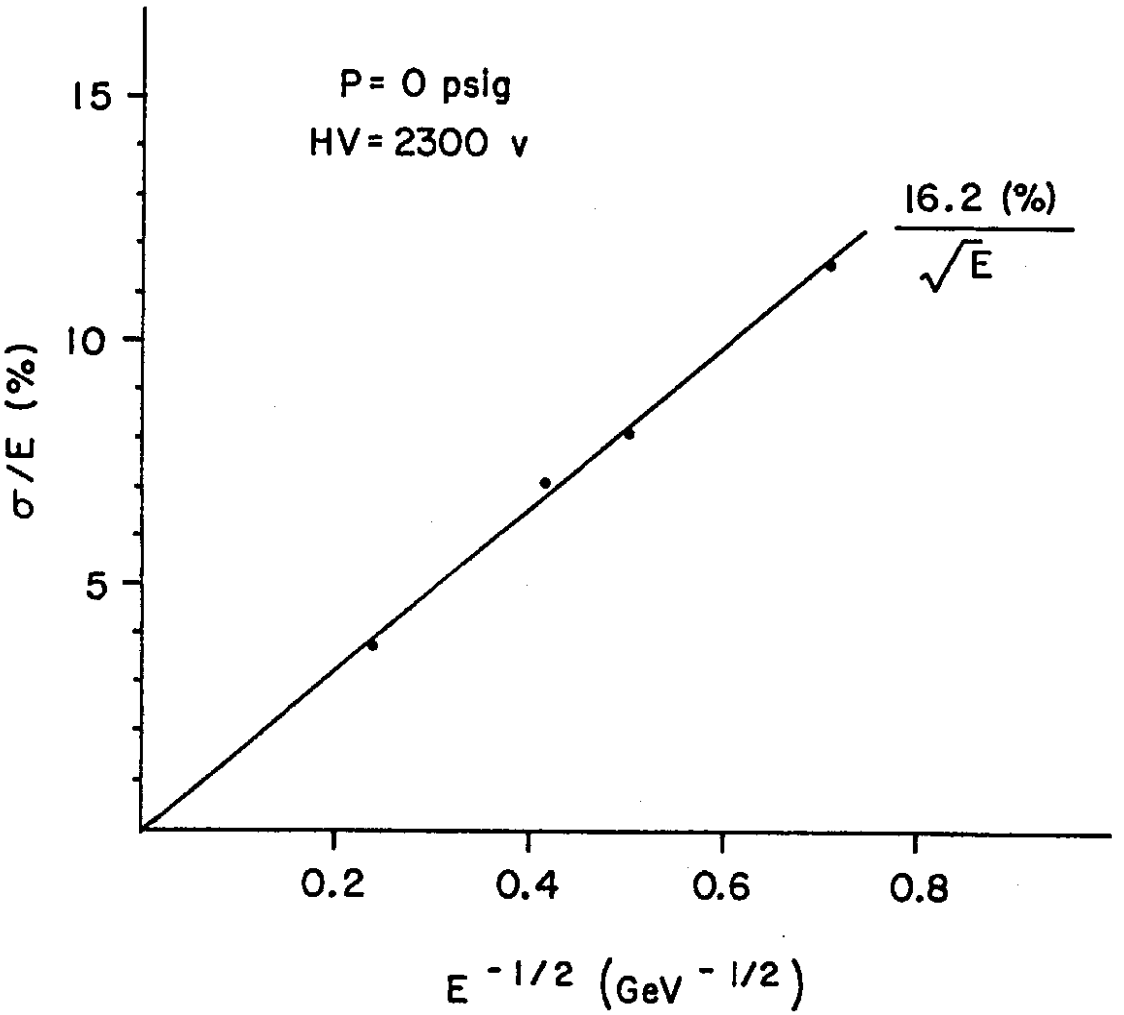

FIG. 14

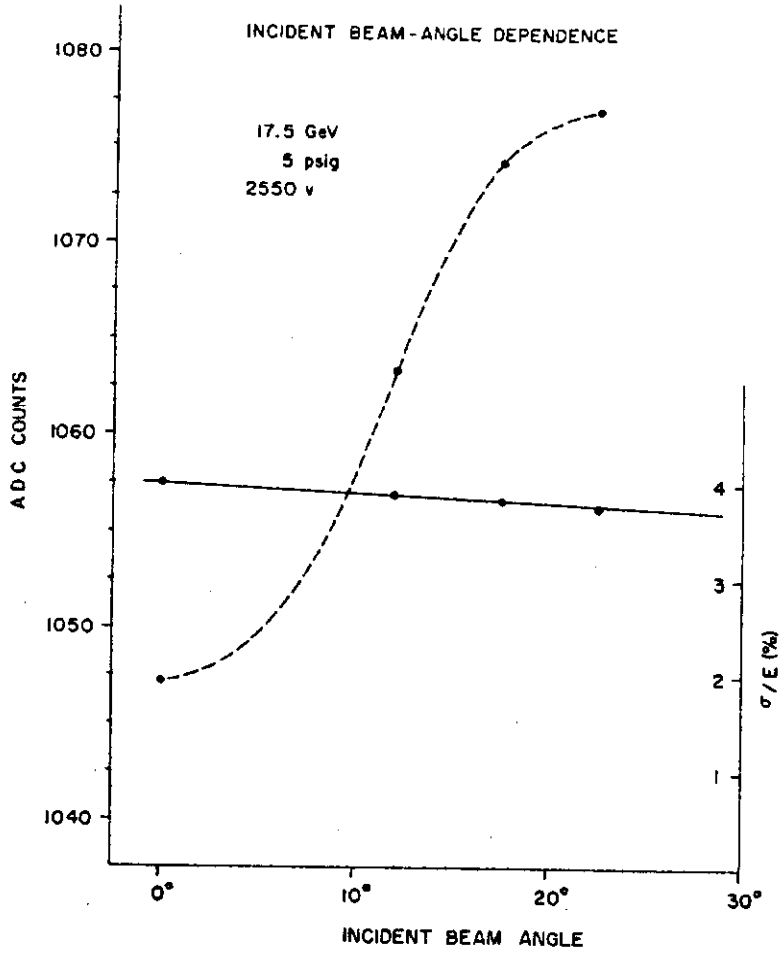
INCIDENT BEAM-ANGLE DEPENDENCE
17.5 GeV
5 psig
2550 v
ADC COUNTS
1080
1070
1060
1050
1040
σ / E (%)
4
3
2
1
0°
10°
20°
30°
INCIDENT BEAM ANGLE

FIG. 15

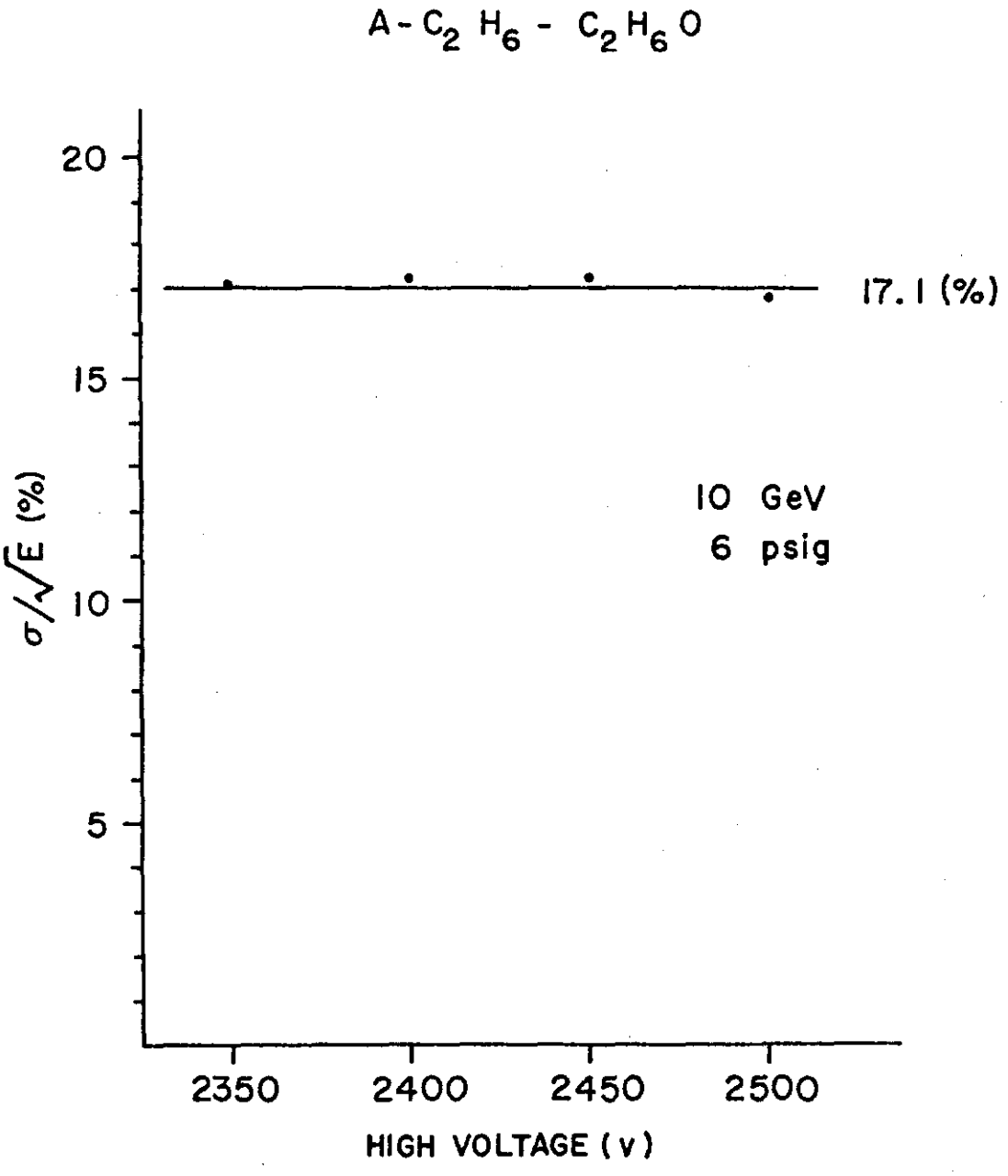
A - $C_2 H_6$ - $C_2 H_6 O$
20
15
10
5
$\sigma/\sqrt{E}$ (%)
17.1 (%)
10 GeV
6 psig
2350
2400
2450
2500
HIGH VOLTAGE (v)

FIG. 16

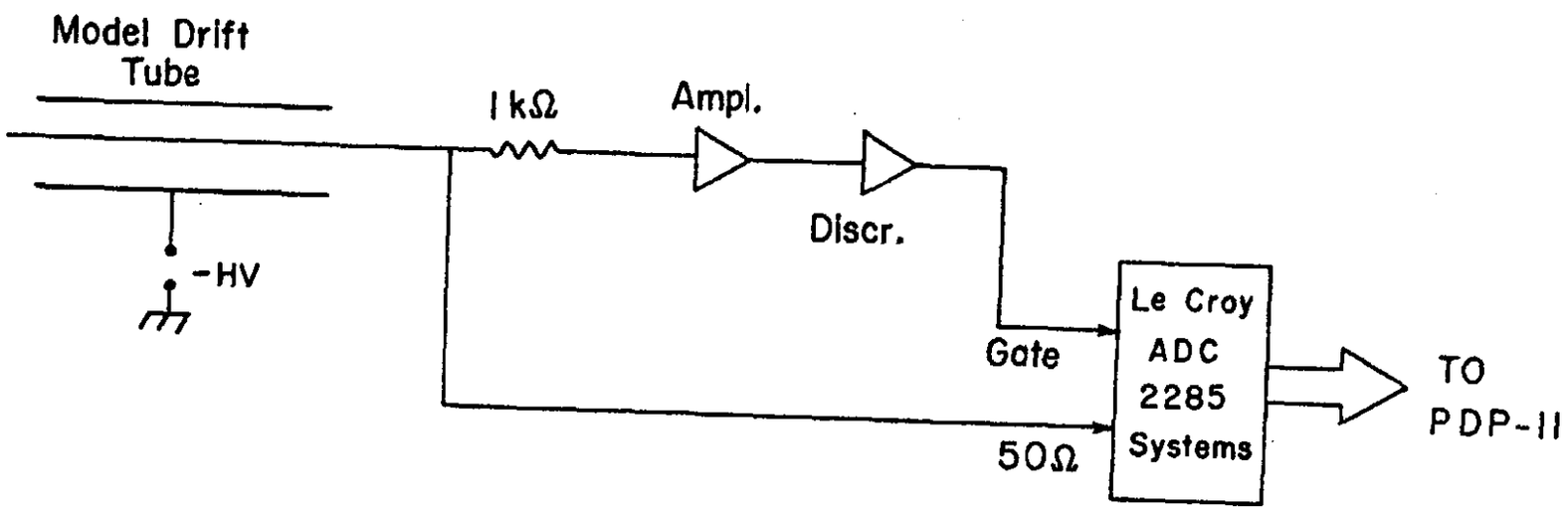
Model Drift
Tube
1 kΩ
Ampl.
Discr.
-HV
Gate
50Ω
Le Croy
ADC
2285
Systems
TO
PDP-11

FIG. 17

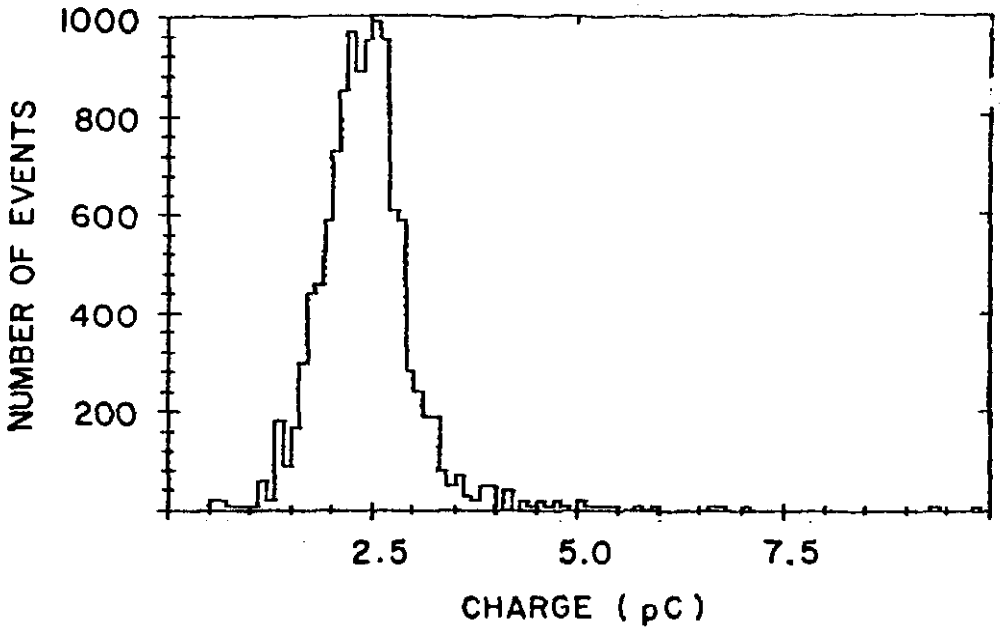

FIG. 18a

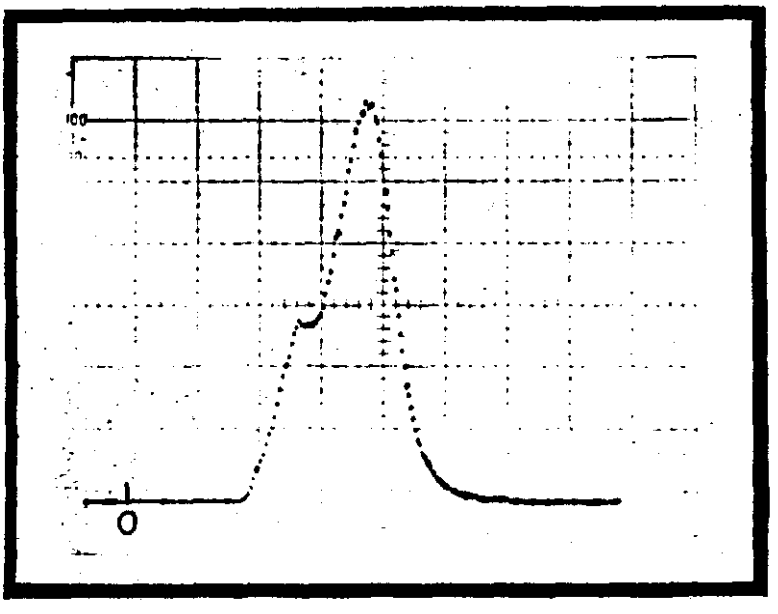

FIG. 18b

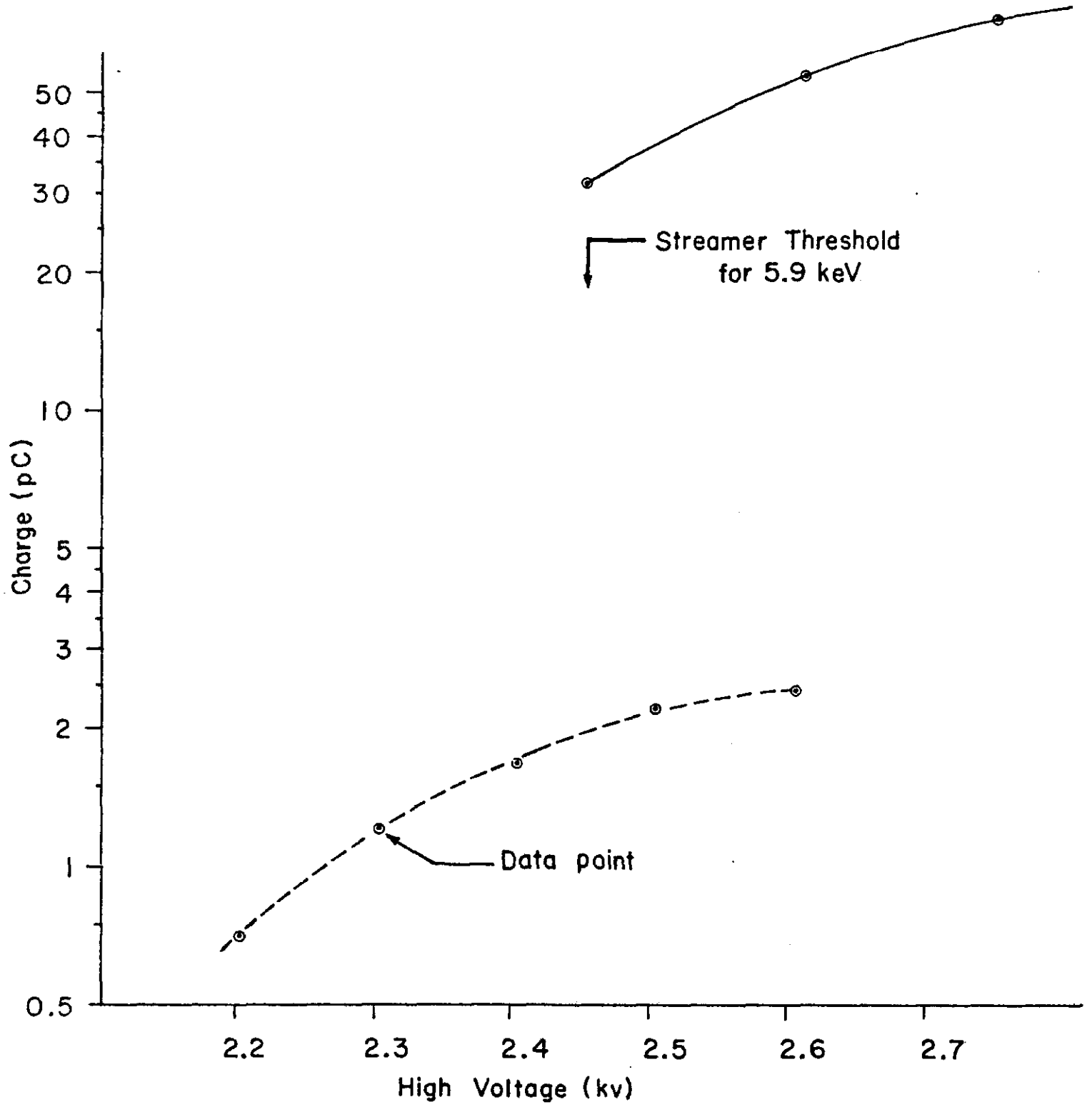
50
40
30
20
10
5
4
3
2
1
0.5
Charge (pC)
Streamer Threshold
for 5.9 keV
Data point
2.2
2.3
2.4
2.5
2.6
2.7
High Voltage (kv)

FIG. 19

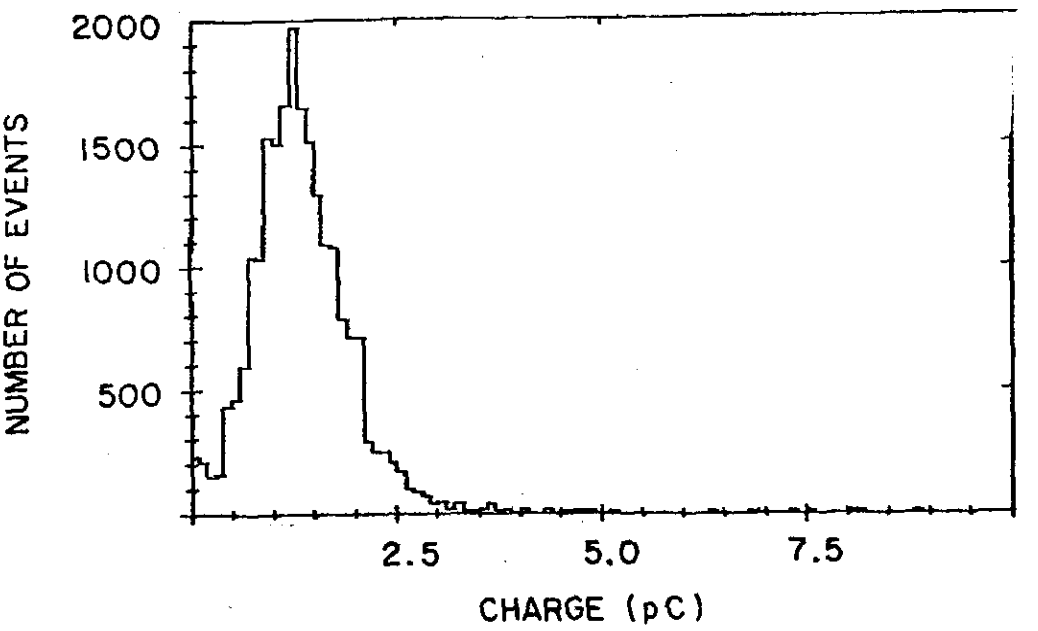

FIG. 20a

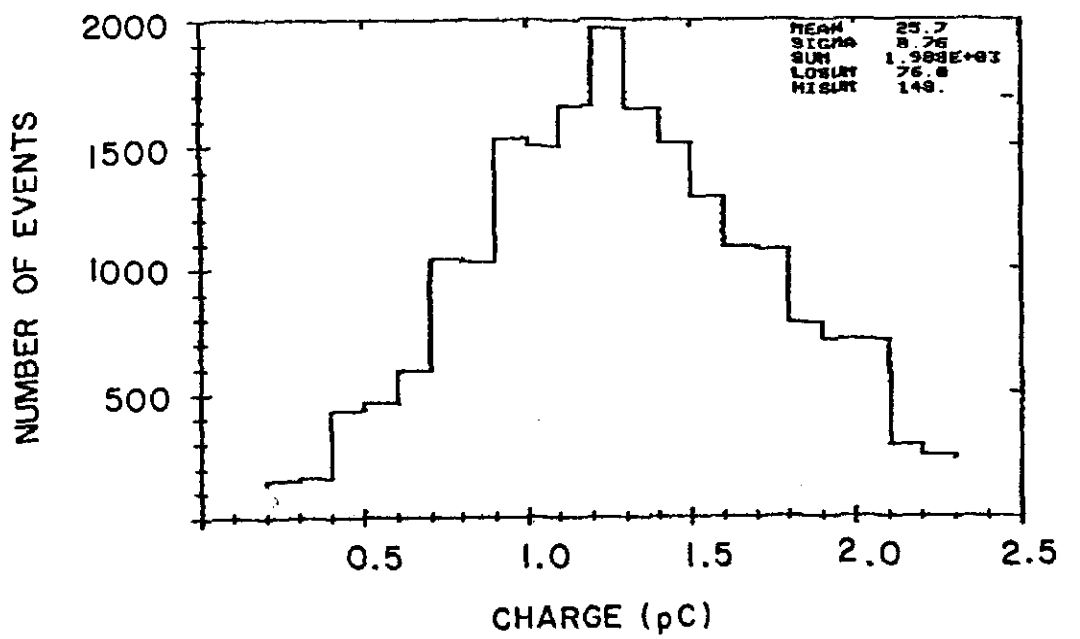

FIG. 20b